Faraday Discussions

Cite this: *Faraday Discuss.*, 2017, **196**, 427

PAPER

A highly sensitive and selective fluorescent probe for hypochlorite in pure water with aggregation induced emission characteristics†

Can Wang, Hongyu Ji, Mengshu Li, Likun Cai, Zhipeng Wang, Qianqian Li and Zhen Li*

Received 9th July 2016, Accepted 28th July 2016
DOI: 10.1039/c6fd00168h

As a reactive oxygen species (ROS), hypochlorite (OCl^-) plays a crucial role in oxidative stress and signal transduction, controlling a wide range of physiological functions. In addition, the wide use of OCl^- in the treatment of food and water might possibly threaten human health if the residual quantity was out of limits. Currently, sensitive methods employed to selectively monitor OCl^- in aqueous samples *in situ* are still scarce and badly needed. Boron esters or acids are considered to be suitable functional groups for the detection of hydrogen peroxide due to their reliable reactivity. In this work, we try to develop a highly sensitive and selective OCl^- probe (**TPE2B**) based on the mechanism of aggregation induced emission (AIE). Due to the distinct increase in water solubility of **TPE2OH**, which is generated from the reaction between **TPE2B** and OCl^-, the strong emission of **TPE2B** is quenched dramatically. The response speed was as fast as 30 seconds with a detection limit as low as 28 nM. Additionally, test papers were also fabricated and exhibited a highly sensitive response to 0.1 mM OCl^-.

1 Introduction

Reactive oxygen species (ROS) are well-known to be crucial to several life functions, and are important signaling molecules and can control a wide range of physiological functions.[1,2] However, surplus creation of ROS would result in oxidative stress and is involved in the pathogenesis of many diseases including cardiovascular diseases, neuron degeneration, arthritis, and cancer.[3–6] Among the various ROS, hypochlorous acid (HOCl) acts as a dominant microbicidal mediator in natural immune systems. The production of HOCl from the reaction of H_2O_2 with Cl^- ions under the catalysis of a heme enzyme myeloperoxidase (MPO) plays a vital role in the ability of cells to kill a wide range of pathogens.[7] Regulated

Department of Chemistry, Wuhan University, Wuhan 430072, China. E-mail: lizhen@whu.edu.cn; lichemlab@163.com

† Electronic supplementary information (ESI) available. See DOI: 10.1039/c6fd00168h

generation of hypochlorous acid is necessary for the host to control the invading microbes, while the HOCl formed can also react with amino acids, proteins, cholesterol, and nucleosides.[8] Moreover, HOCl is used at concentrations in the range of 10^{-5} to 10^{-2} M in the treatment of food preparation surfaces and water supplies in daily life.[9] Such extremely intense hypochlorite solutions are a potential health threat to humans and animals.[10] Thus, it is of great importance to detect hypochlorite through the development of sensitive and selective probes. To this end, a number of methods such as colorimetric,[11] fluorescence,[12] electrochemical[13] and chromatographic methods[14] have been reported. Among these methods, fluorescent probes are undoubtedly one of the most promising tools due to their high sensitivity, good selectivity and non-invasive visualization of biological molecules and processes in live cells and organisms. However, many of them possess relatively complicated structures and are not conveniently synthesized. In addition, plenty of these probes work in mixed solvents containing a large proportion of organic solvent, such as DMF, MeOH and CH_3CN, leading to limited prospects in their practical application. Thus new methods and probes with convenient handling for the detection of HOCl/OCl^- in aqueous solution and in the solid state, such as on test paper, still need to be developed.

It is well known that normal luminogens suffer badly from aggregation-caused quenching (ACQ) effect due to strong π–π stacking interactions, which directly limits their wide applications in aggregated states.[15–18] This phenomenon explains the reason why many reported fluorescent probes work in mixed solvent containing a large proportion of organic solvent. However, the samples to be detected in practical applications are usually in aqueous or even physiological conditions which is inconsistent with the detecting conditions of these conventional ACQ probes. To overcome the adverse impact causing the ACQ effect, researchers have proposed many methods to suppress molecular aggregation.[19] Nevertheless, most approaches are accompanied by adverse effects or need complicated techniques, and facile and effective methods are still rare. In 2001, Ben Zhong Tang's group found the phenomenon of aggregation-induced emission (AIE) for the first time, which is the exact opposite to ACQ observed in conventional fluorophores.[20] The inherent mechanism for this AIE phenomenon is ascribed to the restriction of intramolecular motion (RIM) in the aggregates, which could open the radiative pathway of propeller shaped AIE luminogens, as confirmed from the internal restricted motion of the phenyl ring in silole molecules and their external behavior under different temperatures, in solvents with different viscosity, and under different pressures.[21] In the past decade, a large number of molecules with AIE properties have been reported.[22] Among them, tetraphenylethene (TPE) is the star molecule because of its ease of synthesis and convenience of modification, and has been utilized to construct many good AIEgens as promising candidates for applications in LEDs[23] and sensors[24] *etc.*

So far, a wide variety of substituents have been attached to TPE to endow it with sensing properties.[25–31] Many biosensor probes based on TPE derivatives have been reported, but few probes reported for hypochlorite. On the basis of the AIE mechanism, in this paper we report a highly efficient and selective fluorescent probe for hypochlorite based on the reaction of aryl boronates and OCl^-. The highly hydrophobic **TPE2B** aggregated in a mixture of water and THF (99 : 1, v/v), and the resultant nanoparticles exhibited strong sky-blue emission thanks to its AIE feature. Upon the addition of hypochlorite, the hydrophobic aryl boronate groups were converted to phenol groups and further oxidized to the quinone

form, and accompanied by an increased solubility in water, which resulted in deformation of the nanoparticles and a decrease in fluorescence intensity, as displayed in Scheme 1. The ratio of fluorescence intensity with/without the addition of 50 μM hypochlorite was as high as 376, and the detection limit was as low as 28 nM. Furthermore, other ROS, such as H_2O_2, NO, $^{\bullet}OH$ and *tert*-butylhydroperoxide (TBHP), do not induce an obvious decrease in fluorescence. Moreover, mixing a THF solution of **TPE2B** with water containing OCl^- could effectively distinguish between aqueous samples containing amounts of OCl^- which exceeded the standard (8.4 μM).[32] In addition, test papers of **TPE2B** also exhibited a highly sensitive response toward OCl^- such that the fluorescence was quenched remarkably with a 0.1 mM OCl^- aqueous sample, providing potential application for the solid state detection of OCl^- in the future.

2 Experimental

Materials and reagents

Tetrahydrofuran, toluene and dioxane were dried over and distilled from K–Na alloy under an atmosphere of dry argon. Zinc dust was purchased from Sinopharm Chemical Reagent Co., Ltd and activated with 1.5 M aqueous HCl. 4-Bromobenzophenone, 4-methoxybenzophenone and 4,4′-dimethoxybenzophenone were purchased from Energy Chemical. Diphenylmethane and *n*-butyllithium were purchased from Sigma-Aldrich. Bis(pinacolato)diboron was purchased from Aladdin. *p*-Toluenesulfonic acid monohydrate, boron tribromide, *tert*-butylhydroperoxide, sodium nitroprusside, H_2O_2, NaClO, and all other salts and solvents used in experiments were purchased from Sinopharm Chemical Reagent Co., Ltd. Hydroxyl radicals ($^{\bullet}OH$) were generated from the reaction of Fe^{2+} with H_2O_2. Nitric oxide (NO) was prepared using sodium nitroprusside. Singlet oxygen ($^1O_2$) was prepared using the OCl^-/H_2O_2 system.

Characterization

^1H NMR spectra were recorded on a 300 MHz Varian Mercury or 400 MHz Bruker ARX spectrometer. ^{13}C NMR spectra were recorded on a 400 MHz Varian Mercury

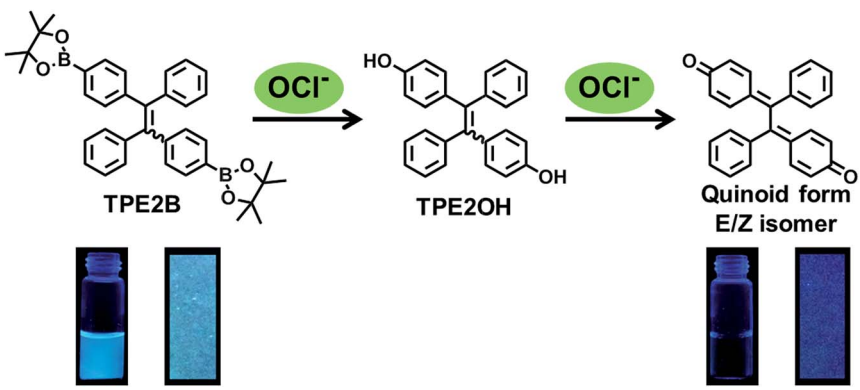

Scheme 1 Schematic illustration for the detection of hypochlorite and photos of the fluorescence change of the probe TPE2B in solution and on test papers on addition of hypochlorite under UV illumination.

or 400 MHz Bruker ARX spectrometer. UV-Vis spectra were measured on a Shimadzu UV-2550. Photoluminescence spectra were performed on a Hitachi F-4600 fluorescence spectrophotometer. High-performance liquid chromatography (HPLC) was performed at ambient temperature on a Shimadzu LC-6AD liquid chromatograph equipped with an ultraviolet-visible detector (320 nm, Shimadzu SPD-20A) and Sepax Bio-C18 (4.6 × 250 mm 5 μm). FTIR spectra were recorded on a PerkinElmer-2 spectrometer in the region of 4000–400 cm^{-1} on KBr pellets. The fluorescence quantum yields (Φ_F) of **TPE2B** in THF/water mixtures with different water fractions were estimated using 9,10-diphenylanthracene (Φ_F = 90% in cyclohexane) as standard. The absorbance of the solutions was kept between 0.04 and 0.06 to avoid the internal filter effect.

Synthesis

TPE2B was synthesized easily from 4-bromobenzophenone using a two-step reaction according to the reported procedure. **TPE2OH**, **TPEB** and **TPEOH** were also synthesized to investigate the sensing mechanism. The general scheme of the synthetic route is illustrated in Scheme S1.†

Synthesis of 1,2-bis(4-bromophenyl)-1,2-diphenylethene (TPE2Br). In a 250 mL Schlenk flask, zinc dust (2.68 g, 41 mmol) in freshly distilled THF (30 mL) was cooled to 0 °C under N_2. $TiCl_4$ (2.2 mL, 20 mmol) was added dropwise to the cold mixture and stirred at 0 °C for 0.5 h. The suspension was warmed to 66 °C and then refluxed for 2 h. After cooling to 0 °C, a solution of dissolved 4-bromobenzophenone (2.61 g, 10 mmol) in freshly distilled THF (70 mL) was added to the suspension and refluxed overnight. After cooling to room temperature, 20 mL hydrochloric acid solution (6 M) was added. The mixture was extracted with CH_2Cl_2 three times. The organic layers were combined and washed with brine twice, then dried over Na_2SO_4, filtered, concentrated, and the crude product was purified on a silica gel column using $CHCl_3$/petroleum ether (v/v = 1/2) as eluent. A white solid was obtained (2.02 g, 82.4%). ^{1}H NMR (300 MHz, $CDCl_3$, δ): 7.24 (m, 4H, Ar–H), 7.12 (m, 6H, Ar–H), 7.00 (m, 4H, Ar–H), 6.88 (m, 4H, Ar–H).

Synthesis of 1,2-diphenyl-1,2-bis(4-(4,4,5,5-tetramethyl-1,3,2-dioxaborolan-2-yl)phenyl)-ethane (TPE2B). To a freshly distilled dioxane solution (20 mL) of **TPE2Br** (0.49 g, 1.0 mmol) was added bispinacolatodiboron (0.61 g, 2.4 mmol), KOAc (0.59 g, 6.0 mmol) and $PdCl_2(PPh_3)_2$ (49 mg, 0.06 mmol) under N_2. The solution was stirred at 80 °C for 18 h. After the reaction mixture was cooled to room temperature, the salt was removed *via* filtration and washed with CH_2Cl_2. The filtrate was then washed with 60 mL water 3 times, and the organic layers were dried over anhydrous Na_2SO_4, filtered, concentrated, and the crude product was purified on a silica gel column using CH_2Cl_2/petroleum ether (v/v = 20/1) to give a white solid of compound **3** (0.44 g, 75.9%). ^{1}H NMR (300 MHz, $CDCl_3$, δ): 7.53 (m, 4H, Ar–H), 7.07 (m, 6H, Ar–H), 7.03 (m, 8H, Ar–H), 1.31 (s, 24H, $-CH_3$). ^{13}C NMR (75 MHz, $CDCl_3$, δ): 147.0, 143.9, 143.8, 143.7, 141.6, 141.0, 134.4, 131.6, 130.9, 127.9, 126.8, 126.7, 83.9, 25.2. IR (KBr) ν (cm^{-1}): 3055 (w), 3024 (w), 2979 (w), 2931 (w), 1947 (w), 1607 (w), 1492 (w), 1444 (w), 1396 (w), 1360 (w), 1321 (w), 1270 (w), 1213 (w), 1088 (w), 1020 (w), 910 (w), 858 (w).

Synthesis of 1,2-bis(4-methoxyphenyl)-1,2-diphenylethene (TPE2OMe). TPE2OMe was synthesized using the same procedure as **TPE2B:** (white powder, 1.96 g, 90.0%).

^{1}H NMR (300 MHz, $CDCl_3$, δ): 7.10–7.06 (m, 10H, Ar–H), 6.93 (t, 4H, Ar–H), 6.64 (t, 4H, Ar–H), 3.74 (s, 6H, OCH_3).

Synthesis of 4,4′-(1,2-diphenylethene-1,2-diyl)diphenol (TPE2OH). To a solution of **TPE2OMe** (1.38 g, 3.5 mmol) in dry CH_2Cl_2 (10 mL), a solution of boron tribromide in CH_2Cl_2 (1.7 mL, 3.6 mmol) was added dropwise under argon at −78 °C. The resulting reaction mixture was stirred at −78 °C for 1 h. The reaction mixture was allowed to warm to room temperature and stirred for another 12 h. The reaction was quenched with the addition of water. The filtrate was washed with de-ionized H_2O three times and dried under vacuum. A white solid was obtained (1.29 g, 98.1%). ^{1}H NMR (300 MHz, $CDCl_3$, δ): 7.10–7.02 (m, 10H, Ar–H), 6.88 (t, 4H, Ar–H), 6.57 (t, 4H, Ar–H), 4.63 (s, 1H, Ar–OH), 4.60 (s, 1H, Ar–OH). ^{13}C NMR (75 MHz, $CDCl_3$, δ): 154.1, 144.2, 139.7, 135.5, 132.8, 131.5, 127.8, 126.3, 114.7.

Synthesis of (2-(4-bromophenyl)ethene-1,1,2-triyl)tribenzene (TPEBr). To a solution of diphenylmethane (3.36 g, 20 mmol) in dry tetrahydrofuran (80 mL) was added 9.1 mL of a 2.2 M solution of *n*-butyllithium in hexane (20 mmol) at −78 °C under nitrogen. The resultant orange-red solution was stirred for 30 min at that temperature. To this solution was added 4-bromobenzophenone (4.18 g, 16 mmol). Afterwards, the reaction mixture was allowed to warm to room temperature and stirred for another 6 h. The reaction was quenched with the addition of an aqueous solution of ammonium chloride. The organic layer was then extracted with dichloromethane (3 × 50 mL). The organic layers were combined, washed with saturated brine solution and dried over anhydrous Na_2SO_4. After solvent evaporation, the resultant crude alcohol (containing excess diphenylmethane) was subjected to an acid-catalyzed dehydration without further purification. The crude alcohol was dissolved in about 80 mL of toluene in a 250 mL round-bottom flask with a condenser. A catalytic amount of *p*-toluenesulfonic acid (570 mg, 3.0 mmol) was added and the mixture was refluxed overnight. After the reaction mixture was cooled to room temperature, the toluene layer was washed with 10% aqueous $NaHCO_3$ solution (2 × 25 mL) and dried over anhydrous magnesium sulfate. Evaporation of the solvent under reduced pressure afforded the crude tetraphenylethene derivative, which was further purified using silica gel column chromatography with petroleum ether as eluent. A white solid was obtained (5.93 g, 90.1%). ^{1}H NMR (300 MHz, $CDCl_3$, δ): 7.20 (d, J = 8 Hz, 2H, Ar–H), 7.09 (m, 8H, Ar–H), 7.04 (m, 6H, Ar–H), 6.89 (d, J = 8 Hz, 2H, Ar–H).

Synthesis of 4,4,5,5-tetramethyl-2-(4-(1,2,2-triphenylvinyl)phenyl)-1,3,2-dioxaborolane (TPEB). TPEB was synthesized using the same procedure as **TPE2B:** (white powder, 780 mg, 83.1%). ^{1}H NMR (300 MHz, $CDCl_3$, δ): 7.54 (d, J = 8 Hz, 2H, Ar–H), 7.04 (m, 17H, Ar–H), 1.31 (s, 12H, CH_3). ^{13}C NMR (75 MHz, $CDCl_3$, δ): 147.02, 143.90, 143.81, 143.73, 141.61, 141.04, 134.35, 131.59, 131.55, 130.95, 127.97, 127.88, 126.77, 126.69, 83.90, 25.16. IR (KBr) ν (cm^{-1}): 3055 (w), 3023 (w), 2978 (w), 2923 (w), 2860 (w), 1607 (w), 1492 (w), 1444 (w), 1396 (w), 1360 (w), 1322 (w), 1269 (w), 1145 (w), 1087 (w), 1021 (w), 858 (w).

Synthesis of (2-(4-methoxyphenyl)ethene-1,1,2-triyl)tribenzene (TPEOMe). TPEOMe was synthesized using the same procedure as **TPE2OMe:** (white powder, 2.62 g, 90.3%). ^{1}H NMR (300 MHz, $CDCl_3$, δ): 7.06 (m, 15H, Ar–H), 6.94 (d, J = 8 Hz, 2H, Ar–H), 6.64 (d, J = 8 Hz, 2H, Ar–H), 3.74 (s, 3H, OCH_3).

Synthesis of 4-(1,2,2-triphenylvinyl)phenol (TPEOH). TPEOH was synthesized using the same procedure as **TPE2OH**: ^{1}H NMR (300 MHz, $CDCl_3$, δ): 7.06

(m, 14H, Ar–H), 6.90 (d, $J = 8$ Hz, 2H, Ar–H), 6.57 (d, $J = 8$ Hz, 2H, Ar–H), 4.60 (s, 1H, –OH). ^{13}C NMR (100 MHz, THF-d_8, δ): 157.1, 145.0, 141.7, 140.2, 135.2, 133.1, 132.0, 128.1, 126.7, 115.1. IR (KBr) ν (cm^{-1}): 3274 (w), 3054 (w), 3023 (w), 1605 (w), 1510 (w), 1492 (w), 1443 (w), 1265 (w), 1171 (w), 1102 (w), 1030 (w), 829 (w).

3 Results and discussion

The UV-visible absorption spectrum of **TPE2B** was measured in a tetrahydrofuran (THF) solution. As shown in Fig. 1a, there are two absorption bands centered at 250 and 321 nm, which are attributed to the π–π* local electron transition of the conjugated system. Compared to that in THF solution, the nanoparticles of **TPE2B**, prepared by mixing 0.1 mL **TPE2B** (in THF) with 9.9 mL water, exhibited an obvious decrease in absorption and broader bands, accompanying with a little hypochromatic shift in the maximum absorption peak. Upon addition of 50 μM hypochlorite (5 equiv.), the color of the aqueous solution changed to faint yellow with a distinctly enhanced absorption band in the range of 350–500 nm. The UV-visible absorption spectrum of **TPE2OH** was recorded to confirm the product upon the addition of NaClO to **TPE2B**. However, compared to the UV-visible absorption spectrum of **TPE2B** treated with NaClO, the spectrum of **TPE2OH** was totally different. Considering the faint yellow color of **TPE2B** after treatment with NaClO, we speculated that the product of **TPE2B** after reaction with an excess amount of NaClO should be the quinoid structure of **TPE2OH**. This was

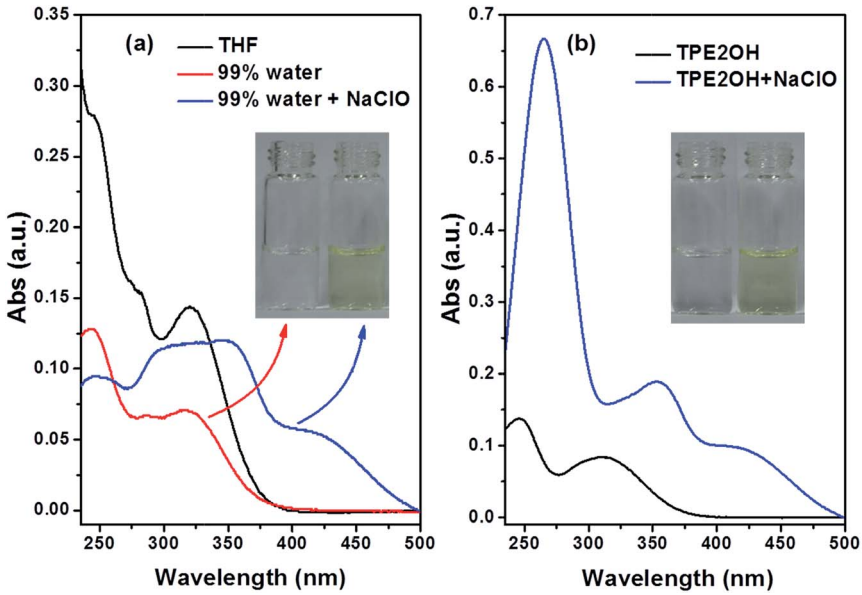

Fig. 1 (a) UV-visible spectra of dilute solutions of TPE2B in THF and in water/THF mixtures ($f_w = 99\%$) with/without the addition of NaClO (5 equiv.). Concentration of TPE2B: 10 μM. The inset depicts images of TPE2B without (left) and with (right) the addition of NaClO. (b) UV-visible spectra of the dilute solutions of TPE2B in a water/THF mixture ($f_w = 99\%$) and with the addition of NaClO (5 equiv.). Concentration of TPE2OH: 10 μM. The inset depicts images of TPE2OH without (left) and with (right) the addition of NaClO.

confirmed from the following experiments. After adding 50 μM NaClO to the solution of **TPE2OH**, the absorption spectrum exhibited a similar enhancement in the range of 350–500 nm.

As it is constructed from a TPE unit, **TPE2B** displays distinct AIE features. As shown in Fig. 2a and b, when the water fraction is lower than 90%, the solution of **TPE2B** is nearly non-emissive ($\Phi_F = 0.01$). However, when f_w is higher than 95%, an emission peak centered at 470 nm appears and is enhanced greatly when f_w is 99% ($\Phi_F = 0.33$). As displayed in Fig. 2c, **TPE2OH** was nearly non-emissive in water/THF mixture ($f_w = 99\%$) and the fluorescence spectrum exactly agreed with that of **TPE2B** treated with 5 equiv. NaClO. The fluorescence quantum yield of **TPE2OH** was also measured with a Φ_F value of 0.01. The following sensor experiments were performed based on nanoparticles of **TPE2B** in a mixture of water/THF ($f_w = 99\%$).

The nanoparticles of **TPE2B** exhibited good photostability upon excitation at 323 nm (Fig. S1†). After the addition of NaClO, its fluorescence was quenched rapidly and reached the minimum in 30 s. This result indicated that **TPE2B** showed an ultra-fast fluorescence response for OCl^-. The change in the fluorescence spectra of **TPE2B** with NaClO at various concentrations was monitored. Fig. 3a shows the fluorescence spectra of the probe **TPE2B** in the presence of different amounts of hypochlorite ions. As anticipated, with the addition of NaClO, the fluorescence intensity of **TPE2B** decreased gradually and the fluorescence was quenched completely with the addition of 50 μM NaClO, while F_0/F was as high as 376. As displayed in Fig. 3b, the fluorescence intensity at 470 nm decreased almost linearly with the concentration of NaClO in the range of 0–30 μM, with a correlation coefficient of 0.9932. Accordingly, the detection limit of NaClO was estimated to be 28 nM (DL = $3\sigma/|k|$, $\sigma = 1.46$, $k = -158.35$). The tremendous quenching ratio value and the perfect linear correlation indicated

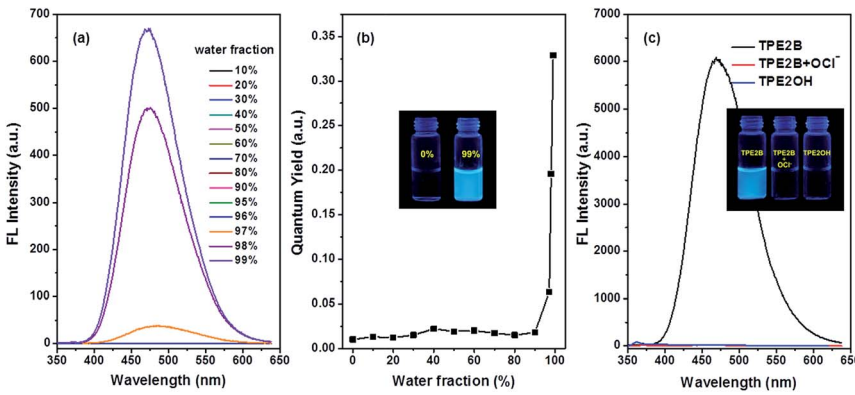

Fig. 2 (a) Fluorescence spectra of **TPE2B** in mixtures of THF/water with an increasing fraction of water. (b) Fluorescence quantum yields of **TPE2B** in water/THF mixtures with different water fractions. The inset depicts the emission images of **TPE2B** in pure THF (left) and a 99% water fraction (right) under 365 nm UV illumination. (c) Fluorescence spectra of **TPE2B**, **TPE2B** treated with 50 μM NaClO and **TPE2OH** in a mixture of water/THF (f_w = 99%). The inset depicts the emission images of **TPE2B**, **TPE2B** treated with 50 μM NaClO and **TPE2OH**. Concentration: 10 μM.

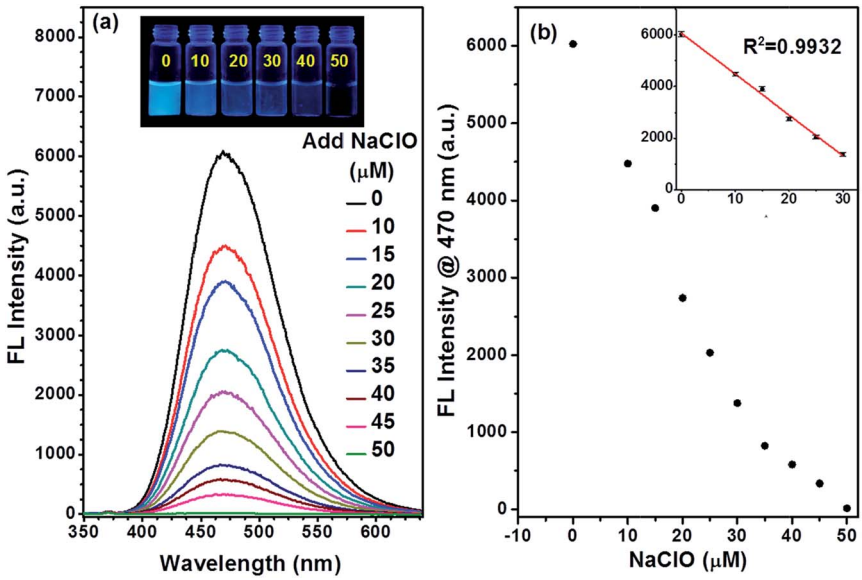

Fig. 3 (a) Fluorescence intensity change of TPE2B (10.0 μM) upon addition of different amounts of NaClO. The inset photos depict the fluorescence response of TPE2B in the presence of different equivalent concentrations of hypochlorite ions. (b) Plot of fluorescence intensity change of TPE2B at 470 nm *versus* varied amounts of NaClO. The inset figure depicts the linear fitting working curve in the concentration range of 0–30 μM.

that **TPE2B** was able to qualitatively and quantitatively determine the level of OCl^-.

To prove the selectivity of **TPE2B** for OCl^-, the fluorescence responses to 28 other kinds of representative species were examined, including common reactive oxygen species (H_2O_2, $^1O_2$, NO, $^{\bullet}OH$ and TBHP). As shown in Fig. 4a, the addition of OCl^- induced a significant decrease in the emissive spectra at 470 nm. For the representative species including H_2O_2, NO, $^{\bullet}OH$, TBHP, I^-, Br^-, Cl^-, F^-, HCO_3^-, ClO_3^-, $Cr_2O_7^{2-}$, HSO_3^-, SO_4^{2-}, HSO_4^-, SO_3^{2-}, CO_3^{2-}, $H_2PO_4^-$, HPO_4^{2-}, PO_4^{3-}, $C_2O_4^{2-}$, Ac^-, IO_4^-, ClO_4^-, IO_3^-, $P_2O_7^{4-}$, NO_3^-, NO_2^- and $S_2O_3^{2-}$, the probe **TPE2B** showed nearly no change in the fluorescence spectra upon addition of these species, indicating that the probe **TPE2B** exhibited a highly selective response towards OCl^- over other anions and reactive oxygen species. It should be noted that the addition of $^1O_2$ also induced an obvious decrease in fluorescence intensity. It should be pointed out that the species $^1O_2$ was prepared by mixing a solution of H_2O_2 and OCl^- in the same concentration. As shown in Fig. 4c, the addition of H_2O_2 did not induce an obvious fluorescence decrease, indicating that **TPE2B** exhibited no response to H_2O_2. When the solution mixture of H_2O_2 and OCl^- was added, the fluorescence intensity at 470 nm was quenched by 70%. The fluorescence was quenched completely upon further addition of an equivalent amount of NaClO. This phenomenon could be explained reasonably. As discussed above, the reaction speed of **TPE2B** with OCl^- was so fast that the reaction could reach its end without stirring in 30 s at room temperature. Thus the fluorescence decrease caused by $^1O_2$ should be attributed to the unreacted OCl^- in the solution

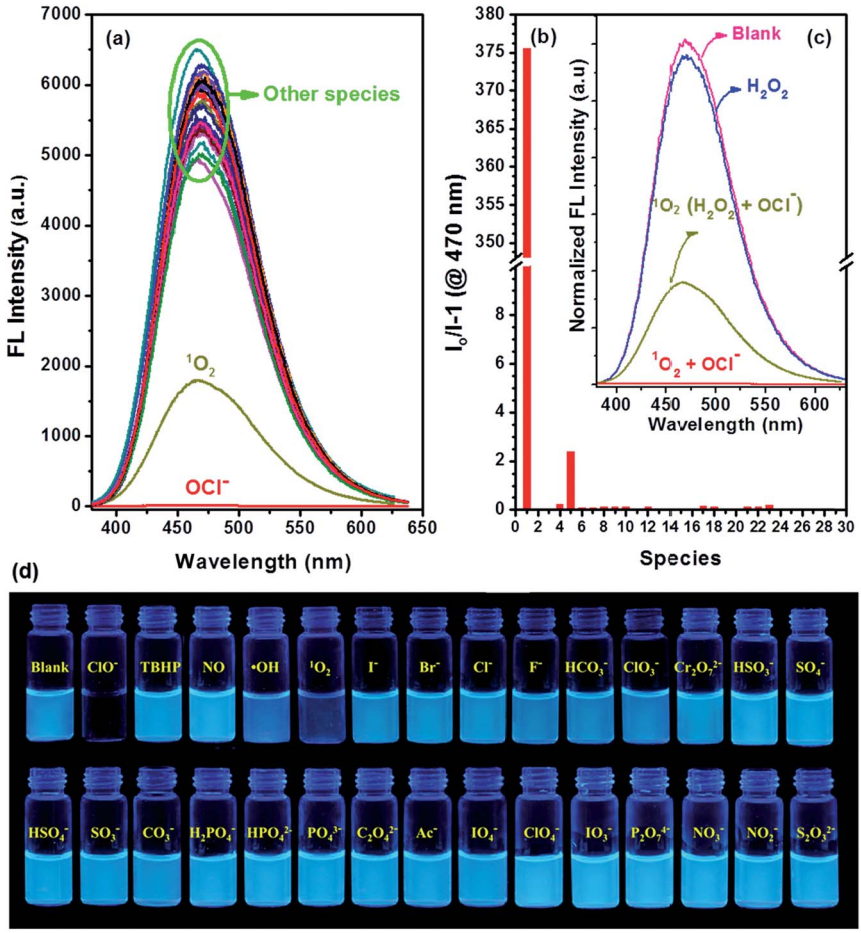

Fig. 4 (a) Fluorescence spectra of **TPE2B** (10 μM) with the addition of 50.0 μM of different species in an aqueous solution (containing 1% THF). (b) Fluorescence response to 50.0 μM of different species. (c) Fluorescence spectra of **TPE2B** (10 μM) on addition of 50.0 μM H_2O_2, 50.0 μM $^1O_2$, and 50.0 μM $^1O_2$ with 50.0 μM NaClO. (d) Emission photos of **TPE2B** upon addition of 50.0 μM of different species under 365 nm UV illumination.

mixture. Additionally, the existence of 5 equiv. of other species did not have an obvious effect on the response of **TPE2B** towards OCl^- (Fig. S2†). The slight interference of I^- was attributed to the I_2 generated from the oxidization of I^- in the air which could react with OCl^-. These results indicated that **TPE2B** achieved a high sensitivity and selectivity in the detection of low concentrations of OCl^- in a practical application.

As we know, it would be more convenient to use such a probe in practical detection cases if the probe could work in the solid state, such as on test papers. Thus, the sensing performance of **TPE2B** on test papers was also performed. A test paper of **TPE2B** was fabricated by dropping a THF solution of **TPE2B** on a filter paper and drying in air for 30 minutes. The sensing behavior was strongly affected by the concentration of the probe solution. A too low concentration of the probe

solution could result in a nice sensing efficiency, but give from a large photobleaching effect, while a too high concentration leads to a poor sensing performance, but less photobleaching. The concentration of **TPE2B** used for the test papers was 0.1 mM, which was optimized from control experiments. As shown in Fig. 5a, the **TPE2B** test paper emitted a strong sky-blue fluorescence under a hand-held UV lamp. After soaking the test paper in water containing OCl^- for 5 minutes, the fluorescence intensity of the test papers decreased significantly with increasing concentration of OCl^-. It is easy to distinguish the fluorescence intensity change at concentrations of OCl^- as low as 0.1 mM with the naked eye. Consequently, the easy-to-prepare test papers can be used to detect OCl^- rapidly and conveniently without resorting to instrumental analysis.

In practical detection cases, the concentration of OCl^- in samples is usually lower than 10^{-5} M. Thus it is very different from common sensing procedures reported in the literature (where a small amount of high concentration OCl^- (millimole degree) is added to the probe solution). However, by taking advantage of the AIE features of our probe, we could realize the sensing procedure at a low concentration (micromolar level). As mentioned above, the probe investigated in this work was prepared by mixing 0.1 mL **TPE2B** (THF, 1 mM) with 9.9 mL water and exhibited strong emission. So, we could mix 0.1 mL solution of **TPE2B** directly with 9.9 mL of aqueous samples to estimate the concentration of OCl^-. The standard work curve of this method was obtained by mixing 0.1 mL **TPE2B** (THF, 1 mM) with 9.9 mL water containing different concentrations of OCl^-. The concentrations of OCl^- were 0, 2.0, 4.0, 6.0, 8.0 and 10.0 μM. A linear correlation was obtained between the fluorescence peak intensity at 470 nm and the

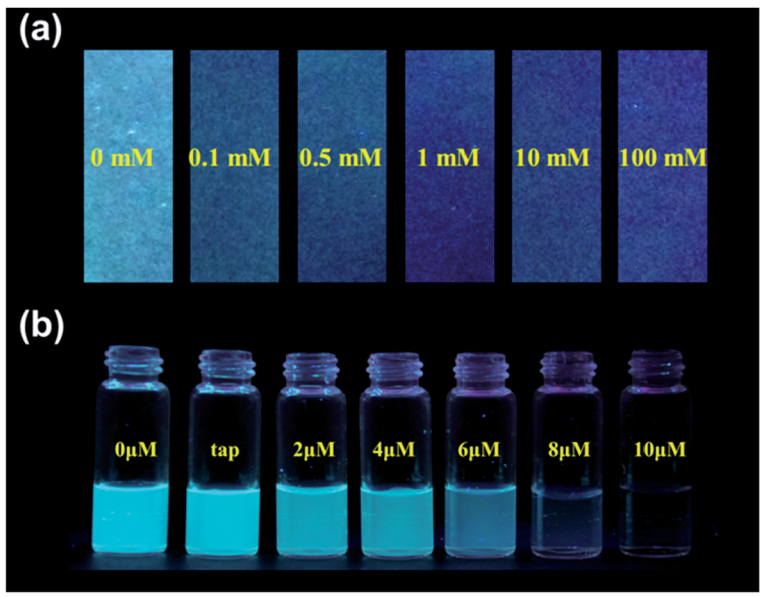

Fig. 5 (a) Emission photos of **TPE2B** on filter papers treated with different concentrations of NaClO under 365 nm UV illumination. (b) Emission photos of **TPE2B** on mixing 0.01 mL **TPE2B** (THF, 1 mM) with 9.9 mL different concentrations of NaClO aqueous solution and tap water, excited using 365 nm UV illumination.

concentration of OCl^- in the range from 0 to 10.0 μM ($R^2 = 0.98$), as shown in Fig. S3.† Based on these results, we applied a standard addition method to determine the concentration of OCl^- in tap water samples. The fluorescence intensity at 470 nm on mixing **TPE2B** (0.1 mL, 1 mM) with 9.9 mL tap water was 3886. According to the equation of linear regression, the concentration of OCl^- in tap water was estimated to be 1.37 μM, which is lower than the required concentration of OCl^- in tap water (8.40 μM). Additionally, as displayed in Fig. 5b, the boundary concentration of OCl^- with/without obvious emission on mixing with **TPE2B** was located around 8 μM, which provided direct evidence from its emission to judge whether the tap water used exceeded the standard for health. These results indicated that this probe has great potential for the quantitative analysis of OCl^- levels in environmental samples and the qualitative judgement of the safety of tap water.

The sensing mechanism of **TPE2B** towards OCl^- was also investigated carefully. The formation of **TPE2OH** after incubation of the probe **TPE2B** with NaClO was confirmed from HPLC analysis. As shown in Fig. S4,† they both exhibited two peaks, attributed to their *E*/*Z* isomers. The retention time of **TPE2B** after treatment with NaClO was largely reduced compared to that of **TPE2B**, and was nearly in accordance with the retention time of **TPE2OH**. The tiny difference should be caused by the quinoid form of **TPE2OH** in the sensing system. As for the existence of *Z*/*E* isomers for **TPE2B**, we synthesized a similar compound **TPEB** to explore the sensing mechanism of the probe. Reaction of **TPEB** with 5 equiv. of NaClO was carried out in water (containing 1% THF). After stirring at ambient temperature for 5 minutes, the product was separated using silica column chromatography and characterized with ^{1}H NMR and FT-IR spectra (Fig. S5 and S6†). The ^{1}H NMR spectrum matched with **TPEOH**, confirming that the product of the reaction between **TPE2B** and OCl^- was **TPE2OH**. The hydrophilic phenol group (actually mostly in the quinoid structure) greatly improved its solubility in water (containing 1% THF), leading to the free rotation of carbon–carbon single bonds between the four peripheral phenyls and the ethylene core, resulting in fluorescence quenching. The fluorescence quantum yield of **TPE2OH** was only 0.01 under this condition.

4 Conclusions

In summary, based on the AIE principle, a highly sensitive and selective probe for the detection of hypochlorite has been successfully designed and synthesized. Apart from its ultra-fast response towards OCl^-, the probe showed no obvious response to other ROS, such as H_2O_2, NO, $^{\bullet}OH$ and TBHP. The detection limit was as low as 28 nM with a 376-fold quenching efficiency towards 50 μM NaClO. Furthermore, test paper experiments were performed to estimate its application in the solid state and a convenient method to evaluate the safety of tap water was developed.

Acknowledgements

We are grateful to the National Fundamental Key Research Program (2013CB834701) and the National Science Foundation of China (No. 21325416, 51573140) for financial support.

References

1 B. C. Dickinson and C. J. Chang, *Nat. Chem. Biol.*, 2011, **7**, 504–511.
2 B. D'Autreaux and M. B. Toledano, *Nat. Rev. Mol. Cell Biol.*, 2007, **8**, 813–824.
3 P. S. Green, A. J. Mendez, J. S. Jacob, J. R. Crowley, W. Growdon, B. T. Hyman and J. W. Heinecke, *J. Neurochem.*, 2004, **90**, 724–733.
4 M. R. Ramsey and N. E. Sharpless, *Nat. Cell Biol.*, 2006, **8**, 1213–1215.
5 N. Houstis, E. D. Rosen and E. S. Lander, *Nature*, 2006, **440**, 944–948.
6 S. Recuter, S. C. Gupta, M. M. Chaturvedi and B. B. Aggarwal, *Free Radical Biol. Med.*, 2010, **49**, 1603–1616.
7 E. Hidalgo, R. Bartolome and C. Dominguez, *Chem.-Biol. Interact.*, 2002, **139**, 265–282.
8 K. M. Wynalda and R. C. Murphy, *Chem. Res. Toxicol.*, 2010, **23**, 108–117.
9 T. Aokl and M. Munemorl, *Anal. Chem.*, 1983, **55**, 209–212.
10 X. Chen, F. Wang, J. Y. Hyun, T. Wei, J. Qiang, X. Ren, I. Shin and J. Yoon, *Chem. Soc. Rev.*, 2016, **45**, 2976–3016.
11 X. D. Lou, Y. Zhang, Q. Q. Li, J. G. Qin and Z. Li, *Chem. Commun.*, 2011, **47**, 3189–3191.
12 L. Yuan, L. Wang, B. K. Agrawalla, S. J. Park, H. Zhu, B. Sivaraman, J. J. Peng, Q. H. Xu and Y. T. Chang, *J. Am. Chem. Soc.*, 2015, **137**, 5930–5938.
13 S. T. Pang, Z. Zhou and Q. M. Wang, *Carbon*, 2013, **58**, 232–237.
14 T. Watanabe, T. Idehara, Y. Yoshimura and H. Nakazawa, *J. Chromatogr., A*, 1998, **796**, 397–400.
15 S. W. Thomas, G. D. Joly and T. M. Swager, *Chem. Rev.*, 2007, **107**, 1339–1386.
16 W. B. Wu, R. L. Tang, Q. Q. Li and Z. Li, *Chem. Soc. Rev.*, 2015, **44**, 3997–4022.
17 Y. N. Hong, J. W. Y. Lam and B. Z. Tang, *Chem. Soc. Rev.*, 2011, **40**, 5361–5388.
18 H. Wang, E. G. Zhao, J. W. Y. Lam and B. Z. Tang, *Mater. Today*, 2015, **18**, 365–377.
19 K. Li and B. Liu, *Chem. Soc. Rev.*, 2014, **43**, 6570–6597.
20 J. Luo, Z. Xie, J. W. Y. Lam, L. Cheng, B. Z. Tang, H. Chen, C. Qiu, H. S. Kwok, X. Zhan, Y. Liu and D. Zhu, *Chem. Commun.*, 2001, **18**, 1740–1741.
21 Y. N. Hong, J. W. Y. Lam and B. Z. Tang, *Chem. Commun.*, 2009, **29**, 4332–4353.
22 J. Mei, N. L. C. Leung, R. T. K. Kwok, J. W. Y. Lam and B. Z. Tang, *Chem. Rev.*, 2015, **115**, 11718–11940.
23 J. Yang, J. Huang, Q. Q. Li and Z. Li, *J. Mater. Chem. C*, 2016, **4**, 2663–2684.
24 L. L. Yan, Y. Zhang, B. Xu and W. J. Tian, *Nanoscale*, 2016, **8**, 2471–2487.
25 Q. Q. Li and Z. Li, *Sci. China: Chem.*, 2015, **58**, 1800–1809.
26 H. B. Shi, R. T. K. Kwok, J. Z. Liu, B. G. Xing, B. Z. Tang and B. Liu, *J. Am. Chem. Soc.*, 2012, **134**, 17972–17981.
27 W. Zhang, W. Liu, P. Li, F. Huang, H. Wang and B. Tang, *Anal. Chem.*, 2015, **87**, 9825–9828.
28 W. Wu, R. Tang, Q. Li and Z. Li, *Chem. Soc. Rev.*, 2015, **44**, 3997–4022.
29 Y. Zhang, X. Huang, W. Liu, G. Zhang, D. Zhang and X. Jiang, *Sci. China: Chem.*, 2016, **59**, 106–113.
30 J. Liang, G. Feng, R. T. K. Kwok, D. Ding, B. Z. Tang and B. Liu, *Sci. China: Chem.*, 2016, **59**, 53–61.
31 X. Ji, P. Wang, H. Wang and F. Huang, *Chin. J. Polym. Sci.*, 2015, **33**, 890–898.
32 Standardization Administration of the People's Republic of China (SAC) has set the drinking water sanitary standard (GB5749-2006), http://www.sac.gov.cn/.

